Chapter 3
Basic NMR Experiments

Abstract In this chapter we shall describe basic NMR experiments used in the fields of Chemistry, Biochemistry and Biology. The topics of acquisition and processing of simple 1D-NMR spectra will be introduced, as well as the fundamental principles behind n-dimensional NMR experiments. For 2D-NMR, some homonuclear and heteronuclear shift correlation experiments based on scalar couplings are shown. The basis of the population transfer that is at the root of heteronuclear experiments is described. The chapter ends with the most relevant nuclear correlations via dipolar couplings, based on the NOE effect.

Keywords Decoupling · Double resonance · Gyromagnetic · Heteronuclear correlation · Multidimensional experiments · Multiple quantum · NOE · Population inversion · Spectral resolution · Signal-to-noise

3.1 Introduction

In the two preceding chapters, we have introduced several characteristics of the atomic nuclei concerning their interaction with a magnetic field, such as nuclear spin, magnetization, chemical shift, spin coupling and relaxation (Chaps. 1 and 2). Although these NMR parameters are very relevant in their own right from a basic physics perspective, in this chapter we are mainly interested in the myriad of applications and experiments that put to use the measurement and interpretation of these key NMR features. The boom in useful experiments in the last decades has ensured the expansion of NMR from its Physics roots into diverse scientific fields like Chemistry, Biology, Materials and Medicine. One of the unique aspects of magnetic resonance spectroscopy compared to other spectroscopic and analytical techniques is the permanent evolution, improvement and development of applications that are specifically tailored to answer new arising questions.

The inherent flexibility of the NMR techniques allows the spectroscopist not only to employ an existing method that might provide the answers sought, but also

R. J. Carbajo and J. L. Neira, *NMR for Chemists and Biologists*,
SpringerBriefs in Biochemistry and Molecular Biology,
DOI: 10.1007/978-94-007-6976-2_3, © The Author(s) 2013

to modify an existing experiment or even *create* a new one that will address the specific problem to be tackled. As a result of this open ingenuity, thousands of different NMR experiments are now on hand that can, to begin with, seem overwhelming to the non-specialist. Several compilations of NMR experiments are available (Berger and Braun 2003; Parella 1999) where some of the most relevant methods are described in detail. Far from such comprehensiveness, our intention here is to provide a general feel for the NMR technique and its potential as analytical tool. In this chapter we shall focus on basic NMR tools applied to molecules in solution. We shall start with the acquisition of typical unidimensional (1D) spectra of some of the most common nuclei (^{1}H, ^{13}C, ^{19}F, ^{31}P) that provide NMR parameters such as chemical shifts and spin-couplings, followed by a description of the origin and applications of two-dimensional (2D) experiments which render more complex and, at the same time, useful information.

3.2 1D NMR

One of the visual representations of data most commonly found in daily life plots the intensity (or variation) of a parameter along an axis. Its simplicity allows an easy and intuitive interpretation of the data, and examples are plentiful: variation of stock values *versus* business hours in finances, ground motion against time during earthquakes as represented in seismographs or evolution of atmospheric pressure throughout the day in weather forecasts. These graphs can be found everywhere in science, and especially in the case of analytical techniques unidimensional (1D) representations are common. Thus, UV and IR spectra show the variation in absorbance *versus* wavelength in nm and cm^{-1}, respectively; Mass Spectrometry presents intensity *versus* mass-to-charge ratio (m/z); and in chromatographic techniques, molecular concentration (usually measured as absorbance) is plotted against retention time (or volume). In the case of NMR, the typical 1D spectrum covers the frequency range (in Hz or ppm) of the nucleus being measured and shows signals at the corresponding chemical shifts for the molecule under study, where the intensity, shape and multiplicity are related to molecular features. The position (i.e. chemical shift or frequency) of each resonance is dictated by the chemical environment of the nuclei (Chap. 2). The magnitude (intensity or integral) of each of the signals correlates with the relative abundance of the nucleus in the molecule under study, and the signal splitting (or its absence!) is a result of the chemical bonds of the nuclei.

3.2.1 Sensitivity and Frequency

Each chemical element in the periodic table has at least one isotope that is NMR active; therefore any nucleus is potentially detectable, but by no means equally

accessible by magnetic resonance (Table 1.2). To compare the ease of measurement of nuclei by NMR, the concept of *receptivity* D^C was introduced:

$$D^C \propto A\gamma^3(I+1)$$

where A and γ are the natural abundance and gyromagnetic constant of the specific isotope, respectively (Table 1.2). The reference receptivity of a nucleus is that of $^{13}C = 1$. Increase in γ value leads to greater sensitivity because of increase in dipolar moment, increased precession rate and augmented energetic transition difference.

Thus, spin $I = ½$ nuclei with high natural abundances and γ (e.g. ^{1}H, ^{31}P, ^{19}F) will not present particular sensitivity difficulties for their detection by NMR in principle. On the contrary, direct NMR detection will be harder for nuclei with very low natural abundance such as ^{15}N ($I = 1/2$, A = 0.37 %, $\gamma = -2.71$, $D^C = 2.19\times10^{-2}$) or nearly impractical if both A and γ are very small as is the case of ^{187}Os, the nucleus with the lowest receptivity ($I = 1/2$, A = 1.96 %, $\gamma = 0.619$, $D^C = 1.43\times10^{-3}$).

From the definition of receptivity, it could be expected that nuclei with quantum spin number $I > ½$ would present a significant sensitivity advantage. However, these $I > ½$ nuclei (also known as *quadrupolar*) have inherent physical properties that give rise to detection problems by NMR (Chaps. 1 and 2). Their broad signals mean low precision in chemical shift and spin coupling measurements and low sensitivity. Therefore, a nucleus like ^{14}N with high receptivity ($I = 1$, A = 99.63 %, $\gamma = 1.93$, $D^C = 5.69$) suffers from a large quadrupolar moment that mars its detection by NMR. Although around 75 % of the nuclei in the periodic table have spin $I > ½$, they have been much less studied by NMR than those of $I = ½$.

The 1D spectrum covers a frequency range for each nucleus that depends on the γ of the isotope measured. If we imagine the whole NMR frequency range available for a 100 MHz spectrometer as a one metre line, ^{1}H will resonate at the end of that line (in the 100 MHz area) covering a region of around 1000 Hz, equivalent to 1 mm of the line (0.1 %). The rest of the nuclei frequencies will be distributed along that metre without overlapping, each of them spanning up to a few mm (i.e. kHz). However, due to hardware and electronic limitations, it is not possible to cover with a single radiofrequency reading or *pulse* the whole range of nuclei, the same way we cannot listen to different radio stations at the same time from a single radio device. Therefore, to acquire the spectrum of our nuclei of interest in a molecule, for example ^{1}H, ^{13}C or ^{31}P, we will need to record an independent 1D experiment for each of them.

The higher the spectrometer field, the longer the line representing the frequencies. However, it is important to bear in mind that, although nuclei will be located always in the same region of the imaginary frequency line relative to each other, their absolute frequencies and range will vary with the spectrometer field; that is, the frequency of the ^{1}H will be always located at the end of the range, but this will correspond to 1000 Hz at 100 MHz and 6000 Hz in a 600 MHz magnet.

This prompted the early NMR community to define the concept of *chemical shift* (Chap. 2). In this way, the NMR spectra of a molecule acquired under identical experimental conditions (solvent, temperature, etc.) but at different spectrometer strength will give identical chemical shift values, with the only difference in the signal resolution due to the larger number of hertz available to define the resonances at higher fields.

3.2.2 Acquisition and Processing

Before we start any NMR experiment it is necessary to tune the probe and to shim the magnet with the sample inside (Chap. 1) (Berger and Braun 2003; Derome 1987; Claridge 1999). Once lock and shims have been finely adjusted, we are ready to acquire our NMR experiments. However, there are several parameters that we will need to adjust/determine in advance to maximise signal-to-noise and resolution. In addition it is worth having post-acquisition protocols to improve the quality of the final spectrum.

3.2.2.1 Signal-to-Noise Ratio (S/N)

We have described previously how to acquire the FID of an experiment (Chap. 1). We know from other spectroscopies that the difference in population between energy levels depends on the Boltzmann constant. In the case of NMR spectroscopy, the energy difference ΔE caused by the magnetic field is very small (1 in 10^5 population difference for a 500 MHz spectrometer and ^{1}H), and directly responsible for the intrinsic insensitivity of the technique. Spectrometer frequency is relevant to ΔE, as increase in magnetic field increase the ΔE gap, and consequently increased population differences. The resolution of an NMR spectrum increases linearly with B_0 and the sensitivity increases with $B_0^{3/2}$, which are the main reasons for the constant technological effort towards higher field magnets. Apart from the field strength, the S/N of the spectrum depends to a large extent on the concentration of the sample, i.e. how many molecules contribute to the NMR signal, where the limiting factor is the availability and/or the solubility of the material. To overcome the low sensitivity of NMR several hardware implementations, acquisition short-cuts and processing "tricks" that improve the sensitivity of the measurements have been introduced over the years.

While other spectroscopies such as UV or IR yield the required information with single-scan acquisitions, such fast experiments are normally insufficient in NMR, and signal averaging is generally required. By accumulating a number n of scans we are adding n spectra on top of each other, with the NMR signal correspondingly increasing n times. However, electrical noise arising from different sources also contributes to the FID, but because noise is inherently random it only increases by $n^{1/2}$. Therefore, the actual gain in S/N after n accumulations is just $n^{1/2}$.

So, in order to double the S/N of a spectrum recorded with 16 scans, we will need four times that number of accumulations (64), with an associated four-fold increase in time. Amongst the several innovations introduced in modern NMR to improve the sensitivity, one of the most successful has been the use of cryogenically cooled probes. These appliances keep the receiver/transmitter coils at very low temperatures (around 70 K) while the sample remains isolated at the measurement temperature of choice, achieving a dramatic reduction of thermal noise in the circuits. Cryoprobes attain a given S/N with fewer scans than conventional ones, and even more importantly, with a concomitant time reduction.

3.2.2.2 Resolution

The quality of a spectrum in terms of its resolution (i.e. the capability of the system to distinguish different frequencies) will depend on factors such as the magnetic field, the number of points allocated to record the FID and the application of post-acquisition processing operations. In terms of resolution, magnets behave like digital cameras, the larger the field (more pixels), the better the spectrum (the picture). A picture taken twice, with four and twelve megapixel cameras, will look similar at the standard $4 \times 6''$ size, but when enlarged the 12 megapixel picture will present a better defined (less pixelated) image. Following the same analogy, the average frequency range for the ^{1}H nucleus spans 10 ppm independent of the field used but that range will cover 2000, 5000 and 9000 Hz in 200, 500 and 900 MHz spectrometers. Thus, at higher magnetic fields more hertz will be available to represent the same NMR signals, and resonances overlapped at low fields will be resolved with more potent spectrometers. Although this resolution improvement might not be that significant for the spectra of simple organic molecules presenting a limited number of resonances, when more complex systems such as biomolecules are studied, signal overlap is significant and the use of high field magnets is mandatory.

The digital resolution of an NMR spectrum also depends on the number of memory points allocated to represent the frequency range. Continuing with the digital camera analogy, the *quality* of a picture (i.e. its digital resolution) is determined by the allocated memory space when it is recorded. In a similar fashion we can acquire the NMR spectrum allocating different number of points, the higher the number the better resolved the frequency domain. This resolution improvement reaches a maximum that is determined by the decay of the NMR signals in the FID, and when the signals have fully decayed the allotment of extra points will just add noise to the final spectrum. Additional points mean an increased acquisition time (larger images take longer times to be stored in the memory card), and the signal may have vanished before the end of the FID recording. In everyday NMR routine, a balance is sought between resolution, memory space and acquisition time. An exception is where signals present fast decay due to short T_2* relaxation times (Chap. 1) where the signal will have disappeared long before the end of the acquisition time. These FIDs will not have

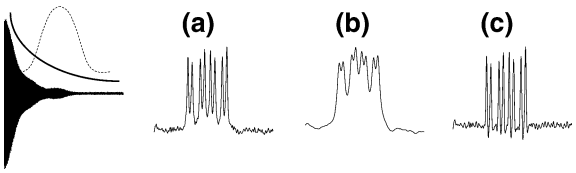

Fig. 3.1 Spectral resolution. Resulting spectra after applying apodization functions to the FID: without apodization (**a**), exponential multiplication to increase sensitivity but with resolution loss (**b**, *full line*) and Gaussian multiplication to improve resolution with a cost in sensitivity (**c**, *dotted line*)

enough frequency information to discriminate individual resonances, leading to broad signals in the spectrum (blurred pictures). Adding acquisition points will not improve the resolution in this case because the magnetization will be fully returned to equilibrium by the time the FID is recorded.

A spectrum can also be enhanced by post-acquisition manipulations of the data (Hoch and Stern 1996). Among the different "cosmetic" methods available, one of the most commonly used is *zero-filling* which consists in doubling the number of points used at acquisition by adding extra points during processing. In this way, digital resolution is increased but there is no penalty on the acquisition time of the experiment because this procedure is applied after the FID has been recorded. Although memory allocation is doubled with zero-filling, it is hardly an issue nowadays in the era of nearly unlimited disk space.

Both signal-to-noise and resolution can be enhanced by several mathematical treatments compiled by the general name of *apodization* or *window* functions. As we have previously seen (Chap. 1), maximum magnetization is observed at the beginning of the FID, which from there decays with time. Therefore, any mathematical operation aimed at increasing the preponderance of the initial points of the FID while at the same time reducing the contribution of the noise-enriched end will yield a gain in signal-to-noise, although at the cost of some loss in resolution (i.e. broader signals) as the frequency information at the end of the FID is diminished. This outcome can be achieved by the multiplication of the FID by a positive exponential function (Fig. 3.1). If the exponential function is applied with negative values, the opposite effect is accomplished: the final part of the FID is enhanced, resulting in an increase in spectral resolution (and noise) at the expense of reducing the beginning of the FID and therefore the part that contributes most to the S/N. This resolution-enhancement processing is achieved with the application of Lorentz-Gaussian multiplications. Other processing functions used for analogous purposes are available in any NMR software, such as the sinusoidal and its squared variant operation or the trapezoidal. Which functions are applied will depend on the information that is needed from a spectrum and it is not unlikely that the same spectrum will be used with different window functions representing different trade-offs.

3.2.2.3 Phasing and Integration

After the successive steps of Fourier transform, zero-filling and apodization, the spectrum is not yet ready for interpretation as it will present non-absorptive resonances. To obtain the final absorption signals, a *phasing* step has to be introduced in the process. The origins of phase errors in NMR spectra are diverse, some of them caused by the fact that the NMR signal is a complex function of real and imaginary (sine and cosine) terms (frequency dependent errors). The instrumentation also plays a part due to phase differences between the receiver and the transmitter. Likewise, due to electronic limitations, the FID cannot be collected immediately after the end of the final pulse in the NMR sequence, and a small delay has to be introduced between those two events. During that delay (commonly 10−1000 μs), magnetization will have precessed to some extent adding extra phase errors to the final spectrum. However, semiautomatic algorithms implemented in modern NMR software packages correct these phase errors and leave the final absorptive signals. Currently, most software allows for a two-parameter phase correction that depends on the particular frequencies of signals.

As seen previously, the NMR spectrum not only contains information regarding the bonding and chemical environment in the form of chemical shift frequencies and *J*-couplings, but quantitative data can also be extracted from the integration of the resonances (Chap. 2). The area underneath each NMR signal is proportional to the number of atoms in the molecule that contribute to it, therefore molecular concentrations can be estimated if a reference of known concentration (e.g. TMS, DSS, TSP) is introduced in the sample. For this method to be accurate, the relaxation of nuclear spins has to be taken into account. If the succession of radiofrequency pulses is too fast, the system is not allowed to recover between scans and fully return to the equilibrium state. Therefore, for the relaxation to be complete, a pre-acquisition delay is introduced prior to the first radiofrequency pulse in order to achieve thermal equilibrium in the system. The duration of the delay (the so-called d1) will depend on the intrinsic relaxation properties of the nucleus to detect. In the case of ^{1}H, for instance, a delay five times longer than the relaxation time T_1 should provide full relaxation, and the concurrent ^{1}H spectrum can be analysed quantitatively.

3.2.3 1D Spectra of ^{1}H, ^{13}C, ^{31}P and ^{19}F

The hydrogen atom is ubiquitous in chemical space and to the advantage of NMR spectroscopists its main isotope ^{1}H presents very favourable physical properties for its detection: spin ½, nearly 100 % abundance and the highest sensitivity of the whole periodic table with a receptivity D^{C} nearly 6000 times that of ^{13}C. Not surprisingly, the ^{1}H signal of H_2O was the first NMR spectrum recorded, and 1D ^{1}H experiments are a major part of day-to-day routine NMR in chemistry labs. Its importance is exemplified by the fact that spectrometer strength, at least in the

chemistry/biology areas, is described by the frequency at which the ^{1}H nucleus resonates (e.g. 500 MHz) and not by the SI unit of magnetic field, the tesla (T). A basic 1D ^{1}H experiment and the corresponding outcome for the cholesterol molecule are represented in Fig. 3.2a. Basically, the design of the 1D pulse sequence consists of a pre-acquisition delay (the d1 described above) that allows the establishment of equilibrium conditions between consecutive scans. This brings magnetization parallel to the magnetic field along the z axis. The d1 delay is followed by a pulse of radiofrequency applied with the carrier at the middle of the ^{1}H chemical shift range (Chap. 1), allowing the excitation of all proton frequencies at the same time. The effect of this pulse is to tilt the ^{1}H magnetization by an angle θ (commonly 90°), with its corresponding projection on the xy-plane being detected as a FID while it decays during the time t. This pulse sequence can be repeated indefinitely and the collected FIDs added as many times as necessary to achieve the desired S/N. After the application of processing and further embellishment using the methods described in the previous section, the 1D ^{1}H is ready for analysis and interpretation.

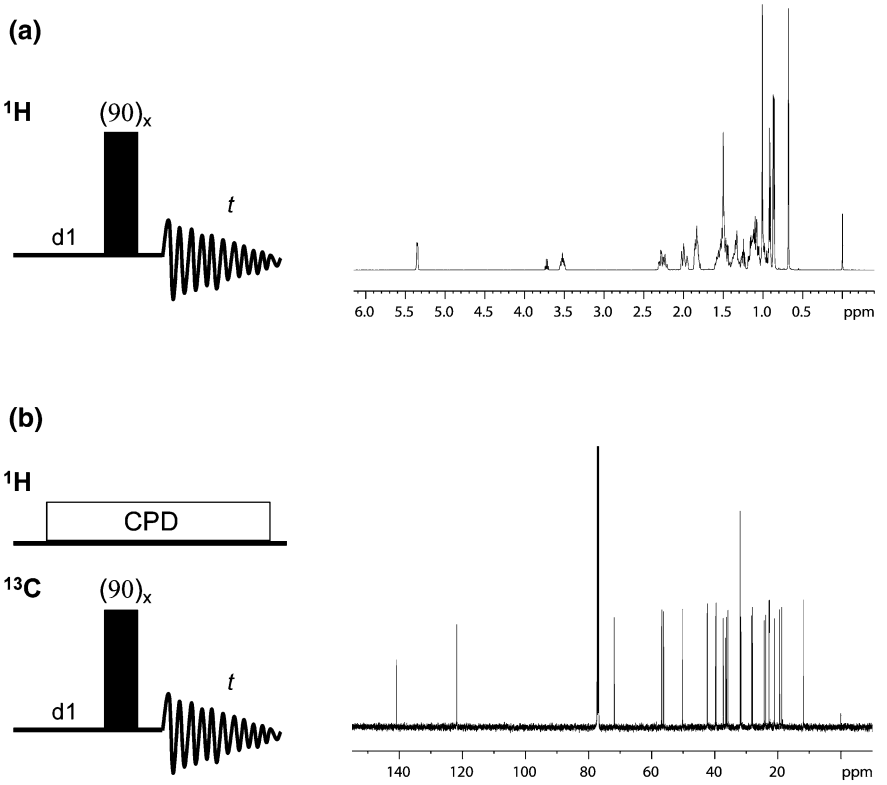

Fig. 3.2 1D NMR. **a** Standard ^{1}H NMR pulse sequence and ^{1}H spectrum of cholesterol (solvent $CDCl_3$). **b** Standard ^{13}C NMR pulse sequence and ^{13}C spectrum of cholesterol (solvent $CDCl_3$)

Carbon is also a ubiquitous element in nature, and therefore of the highest significance in chemistry and biology. Unfortunately for NMR spectroscopists, its most abundant isotope ^{12}C has null spin and therefore cannot be detected with this technique. Its measurement is possible thanks to the ^{13}C isotope, which presents spin ½ but merely 1.1 % of natural abundance. Sensitivity-wise, this number entails that only one out of every 100 molecules in the NMR tube will contribute to the ^{13}C spectrum, or if seen from a sample concentration perspective, a 1 mM sample will see its ^{1}H signals at 1 mM, but its ^{13}C atoms will be at a concentration of just 10 μM. We have described previously (Sect. 3.2.1) that the sensitivity of any nucleus depends also on its gyromagnetic ratio and in the case of ^{13}C its γ is ¼ that of ^{1}H. Therefore, disregarding natural abundance ^{13}C is ab initio four times less sensitive than ^{1}H, with a final relative sensitivity of $1.6x10^{-2}$ when natural abundance is taken into account. If sample availability is not an issue, good quality ^{13}C spectra can be obtained in a matter of a few hours or even less, but if there is a limitation of sample amount (μM range or below), the same task could take a prohibitive amount of time. These sensitivity issues regarding ^{13}C detection, also shared with other low sensitivity nuclei, have been partly alleviated through different improvements in hardware, such as the aforementioned cryoprobes or nano/microprobes, which use very small volumes of sample (a few microliters instead of the typical 0.5 mL) thereby making higher concentrations of sample possible where sample amounts are limiting. In the case of biomolecular NMR (Chap. 4), where the use of multidimensional and multinuclear experiments is common, these hardware implementations are not sufficient to detect insensitive nuclei such as ^{13}C (or ^{15}N), and isotope labelling of the samples is routinely practiced to achieve high levels of $^{13}C/^{15}N$ incorporation.

From an experimental point of view, a typical 1D ^{13}C experiment is acquired in a similar fashion to a ^{1}H spectrum, with the application of a short pulse at the frequency of the ^{13}C nucleus followed by the FID recording (Fig. 3.2b). A pre-acquisition delay d1 is included as well, normally of longer duration than for ^{1}H experiment, as the ^{13}C nuclei present much longer spin-lattice relaxation rates and therefore need extended times to achieve the full return to equilibrium. The ^{13}C is normally acquired with the application of ^{1}H decoupling throughout the whole pulse sequence. This broadband decoupling is accomplished via composite pulse decoupling (CPD, Sect. 3.5.3) with two main purposes: first, a sensitivity enhancement through the elimination of the splittings due to the ^{1}H-^{13}C couplings, yielding singlets for all the ^{13}C resonances independently of the number of hydrogens bound to the carbon; and second, the decoupling produces a NOE effect (Sect. 2.3.1) on the carbon from the attached Hs that also translates into an enhancement of the ^{13}C signal. For this reason, quaternary carbons present very low sensitivity in the ^{13}C spectra, as they do not receive this NOE effect, together with their longer relaxation times due to the absence of directly bound protons (and so, the absence of nearby dipole–dipole interactions). As an example, the ^{13}C spectrum of cholesterol is shown in Fig. 3.2b. The frequency range for the ^{13}C nucleus spans for over 200 ppm, and the overlap of signals is therefore less prevalent than in ^{1}H spectra (Chap. 2, Fig. 2.3b).

Analogous to the ^{1}H nucleus, chemical and bonding information can be readily extracted from the chemical shift of the ^{13}C signals applying the rule that correlates higher frequencies with increased electronegativity. Regarding coupling information, the low natural abundance of ^{13}C implies that ^{13}C-^{13}C splittings will not be observed due to the extremely low probability of finding a ^{13}C bound to another carbon-13 neighbour in all the molecules in the sample. Although the ^{1}H-^{13}C coupling is normally suppressed for sensitivity reasons (see above), the multiplicity information can be recovered by turning off the ^{1}H decoupling during the FID recording, in an experiment known as *gated decoupling*. However, this experiment suffers from very low sensitivity as the only remaining S/N enhancement on the ^{13}C signals will arise from the NOE effect produced by the ^{1}H decoupling during the d1+pulse time. Nevertheless, equivalent multiplicity information can be obtained in a more rapid and intuitive way using ^{13}C-edited experiments such as DEPT (Sect. 3.5.1). A complementary version of the gated decoupling experiment (decoupling *off* during d1+pulse, *on* during *t*) is used when quantitative measurements of ^{13}C are required. With this experimental setup the NOE contribution due to the protons bound to the carbon is eliminated and signal intensity will be exclusively ascribable to the ^{13}C natural ratio, bearing in mind that for quantitative results much longer relaxation delays will be required to achieve full recovery of the ^{13}C magnetization.

Although any element of the periodic table can theoretically be measured via 1D NMR experiments, only those with relevant interest in chemistry and/or biology that present high natural abundances and sensitivities are normally measured. Among these nuclei are ^{31}P and ^{19}F, both of spin ½ and 100 % natural abundance (Table 1.2). Their high sensitivity allows the acquisition of 1D spectra in just a few minutes, covering ranges of several hundred ppms for each of the two nuclei. The interpretation of the chemical shift variation follows the rules described for ^{1}H and ^{13}C, although in the case of ^{31}P the oxidation state of the nucleus has a notable influence that has to be considered for comprehensive interpretation. Experimentally, both ^{19}F and ^{31}P can be acquired with or without ^{1}H decoupling, but as there are no sensitivity issues regarding their detection, a non-decoupled spectrum provides extra information such as the $^{19}F/^{31}P$-^{1}H *J* couplings that can be very valuable for the structural analysis of the molecule under study. ^{31}P presents an interesting characteristic related to its relaxation which is dominated by the chemical shift anisotropy mechanism (CSA) (Chap. 1). The CSA mechanism is field-dependent, and in those nuclei where it prevails the relaxation will be faster at higher fields, which can lead to broader signals. Thus, opposite to what logic would tell us, in the case of the ^{31}P detection the experiments will see an improvement both in S/N and precision with increasing spectrometer frequency but up to a certain magnetic field (around 500 MHz) above which the quality of the ^{31}P spectra declines due to the CSA relaxation dominance. Thence, higher magnetic fields (and higher costs!) are not always the best recipe for experimental success.

3.3 Multidimensional NMR

From the distance, the skyline profile of a big city like New York is largely dominated by its characteristic huge skyscrapers. That view makes the impression of the buildings being aligned side by side to each other. However, those buildings are actually located at different distances from the Manhattan shores and it is difficult to determine which buildings are closer to the observer with the only information provided by the skyline profile. In addition small buildings situated behind large ones are not visible in the profile view. Everyone would therefore agree that a skyline picture is not the best option to navigate through the streets of any city, and that a map would be a much better option. Returning to NMR, the 1D NMR spectrum is our skyline picture of a molecule, where instead of buildings we have resonances, and in place of connecting streets we have chemical shifts and *J*-couplings linking atoms. When molecules increase in size and structural complexity, more resonances will appear in the 1D spectrum and as the chemical shift range for ^{1}H is limited, some overlap will be unavoidable, with smaller signals disappearing underneath more intense ones, that hindering direct analysis of chemical shifts or couplings. In NMR, the *maps* to navigate through the spectra are multidimensional experiments, as the extra dimensions help to unravel the signal overlap and highlight connectivities. In these *n*D experiments, there is a main horizontal dimension that normally is occupied by the ^{1}H frequency range, while the extra added dimensions are constructed from the scalar and dipolar coupling connections between protons and any other nuclei within the molecule. In this section of the chapter, the basic principles to produce the second or any additional dimension in NMR will be introduced, as well as a description of some of the simplest multidimensional experiments, which are the building blocks of all the n-dimensional ones. In the following sections we will discuss some of the most popular 2D experiments, describing the kind of information they yield without going into much detail of the physics, differentiating those based in chemical bond connections such as COSY, TOCSY or HSQC from those based on dipolar couplings like NOESY.

3.3.1 Generating Dimensions in NMR

Every multidimensional NMR experiment follows the simple block scheme depicted in Fig. 3.3, with four differentiated stages: *preparation-evolution-mixing-detection*. The *preparation* stage is common to the 1D experiments described before, and includes any pre-pulse relaxation delay for the system to return to equilibrium between scans and the initial radiofrequency pulse or pulses applied to start tilting the magnetization. It is during the *evolution* stage where the multidimensional experiment is mainly fabricated. Although radiofrequency pulses can also be included during this stage, the most relevant parameter during the

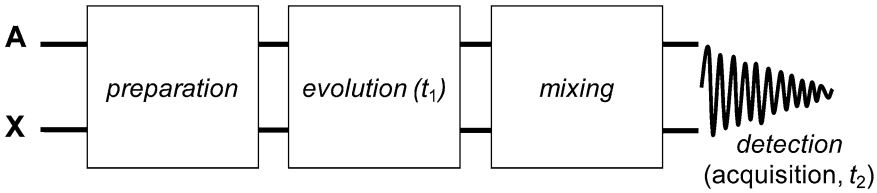

Fig. 3.3 Multidimensional NMR. Representation of a generic multidimensional NMR experiment correlating nuclei A and X. Any n-dimensional NMR experiment can be divided into four stages: *preparation*, *evolution*, *mixing* and *acquisition*. Several pulses and delays can be included into each of the stages. The convention is to represent the evolution time that gets incremented during the multidimensional experiment by t_1, whereas t_2 is the fixed acquisition time

evolution part is the incremental time t_1. The particularity of this time versus other fixed delays such as d1 is that t_1 "evolves" during the experiment, being incremented as the NMR experiment progresses. The first FID will be recorded with the shortest t_1 in the same way as any other 1D spectrum, but the following FIDs will have a total *evolution time* of $t_1 = t + n\mathrm{d}$, where t is the starting evolution time, d is a fixed short delay and n goes from 1 to the number of FIDs we want to record to create the second dimension (number of FIDs = number of points defining the 2nd dimension). Therefore the first and last FID of a 2D experiment will have evolution times of very different lengths (we shall return later to the experimental consequences of the inclusion of an incremental delay during the sequence). The third stage within our multidimensional experiment is called the *mixing*, and during this section of the experiment that can include several pulses and short and/or long fixed delays, the magnetization is modulated in such a way that it will render observable and interpretable information in the resulting spectrum. The last stage consists on the *detection* of the NMR signal generated along the previous steps, following the same methodology described for the 1D experiment: recording of the FID during a fixed delay (t_2) with or without simultaneous decoupling of any of the nuclei participating in the pulse sequence.

We shall now try to explain the involvement of the incremental time t_1 in the generation of the second dimension in a multidimensional experiment simply. The initial preparation stage is equivalent every time the magnetization goes through it; therefore the state of the spins at the beginning of the evolution period will be always the same. At this point we can think of the magnetization as being "labelled" with chemical shift and coupling "tags", but not yet ready to be "read". The first time magnetization goes through the evolution period, these tags will evolve during t_1 in a certain way, reaching the mixing period where they will be further transformed into a "readable" mode (the NMR signal) that is detected during the FID recording. If the Fourier Transform (FT) is applied at this point, we would obtain a 1D spectrum that corresponds with the first dimension of our multidimensional experiment. The second time we go through the pulse sequence, we will arrive at the evolution period with the same magnetization labelled with the same tags we got the first time around. However, during the second pass

through the evolution period t_1 will be slightly incremented (the size of that increment is not relevant for our discussion), and the tags will have some extra time to evolve resulting in magnetization that enters the mixing period in a different state to the first time. The FT of this second FID will yield another 1D spectrum, but with incremental differences to the one recorded before. This process will be repeated n times with t_1 getting incremented nd with every step, resulting in n different FIDs. At the end of the 2D acquisition we shall have n FIDs recorded with N points that if processed will generate n 1D spectra. The second dimension is produced by selecting the first of the N points for each of the n FIDs and applying to them a second Fourier Transform, then the second point, the third, etc., till we have applied as many FTs as N points we have used to define the first dimension. The number of FIDs recorded, n, will determine the number of points we can use to define this second dimension. We define the real transformed dimension as f_2 (FID recorded during t_2) and that obtained by the increment of t_1, the f_1 dimension.

3.3.2 2D Data Acquisition and Processing

The basic tools already described in the acquisition and processing of unidimensional experiments (Sect. 3.2.2) are also applicable for the multidimensional ones. However, some aspects regarding the resolution of multiple dimensions have to be taken into account. A 2D experiment (n FIDs) will have a longer duration than the normal 1D spectrum (one FID), if keeping the number of scans constant. However, we can save acquisition time by reducing the resolution in both dimensions, which is not as crucial as in 1D experiments. For a 2D experiment a typical number of points would be 2048 (2K) for the first dimension (f_2) and 128 points for the second one (f_1), which would be equivalent to the recording of 128 1D spectra of 2K points each. The level of sensitivity needed to observe signals is defined by the number of scans applied to each FID, and considering that each acquisition normally takes a few minutes, the total 2D experimental time will be the result of those few minutes $\times$ 128. If higher resolution is needed in the second dimension (e.g. 256/512 points), the total experimental time will increase accordingly. In order to obtain higher dimensionality spectra (3D, 4D, and so on), additional incremental times are introduced in the pulse sequences, with each extra dimension needing a number of defining n points with the consequent increase in acquisition time. So while a typical 1D spectrum can last just a few minutes and a simple 2D can easily consume a few hours, 3D experiments need acquisition times in the order of days. Although improvements in hardware sensitivity or shortcuts in the acquisition/processing area have been implemented recently, it is evident from the above that multidimensional NMR spectroscopy is still a very demanding technique time-wise. Also, any extra dimension brings about an increase in the size of the recorded data that translates into increased memory allocation for each experiment (about ½ Gb for a typical 3D experiment).

We can distinguish homonuclear (same nuclei in all dimensions, normally ^{1}H) and heteronuclear (different nuclei in different dimensions) experiments. In the case of the ^{1}H homonuclear experiments, the irradiation frequency is situated in the middle of the chemical shift range of the proton, and matched spectral widths (SW) are used for all dimensions. When observing different nuclei, adequate tuning of all frequencies affected has to be done in advance, and the SW and irradiation frequency of the heteronuclei established. The latter is not a superfluous task, as the large chemical shift ranges that some nuclei require cannot be completely covered with a single radiofrequency pulse. In these cases several 2D experiments are recorded shifting in each one the irradiation frequency of the heteronucleus, covering the whole range of possible chemical shifts in this way.

As we have explained before, the resolution of a multidimensional spectrum is determined by the number of points used to define each of the participating dimensions. However, this resolution is not written in stone and can be improved a posteriori using similar tricks to those described for 1D NMR. Thus, zero-filling is normally applied in all dimensions to improve spectral resolution without a penalty in acquisition time. Another interesting mathematical operation often applied in multidimensional NMR is *linear prediction* (mathematical operation where future values of a discrete-time signal are estimated as a linear function of previous samples). In a nutshell, this operation extrapolates points at the beginning (backward) or at the end (forward) of the FID based on the actual recorded data. Therefore it adds unrecorded points to the FID, i.e. resolution, without any acquisition-time cost. However, linear prediction must be applied carefully and overuse should be avoided, bearing in mind that resolution enhancement needs a good starting S/N or it may easily lead to the generation of spurious signals.

3.4 Homonuclear Shift Correlation: Correlations Through the Chemical Bond

As the name indicates, homonuclear experiments are constructed using the same nuclear frequency, usually the ^{1}H, in all dimensions. In principle, any other nucleus could be subjected to this kind of experiment, but either their low sensitivity (e.g. ^{13}C) or the reduced number of atoms within the molecule (e.g. ^{31}P, ^{19}F) makes them much less useful than the ^{1}H variants. In the following section we describe homonuclear correlations such as COSY and TOCSY that make use of J_{HH} scalar couplings to connect protons within the molecule, and secondly briefly outline homonuclear methods such as INADEQUATE that are applied for the correlation of low-abundance nuclei.

3.4.1 COSY. Experiment Interpretation and Practical Aspects

The COSY (COrrelation SpectroscopY) sequence was the first multidimensional NMR experiment described. It was proposed by Jeener at a conference in 1971 (Jeener 1971), although its practical implementation took a few more years due to technical issues (Aue et al. 1976; Bax and Freeman 1981). Figure 3.4a shows the pulse sequence for the simplest COSY experiment and a representation of the kind of signal correlation we expect from this experiment. The basic COSY sequence presents only two 90° radiofrequency pulses separated by the incremental time t_1. With the first pulse (*preparation* stage) magnetization will turn from the equilibrium state in the z-axis to the xy-plane, giving rise to the *evolution* phase where spins develop chemical shifts and homonuclear coupling connections during t_1. The second 90° pulse (*mixing* block) converts this information into magnetization that can be analysed. The diagonal signal correlates each proton (or any other nucleus used in the COSY) with itself and therefore provides no structural or bonding information. The interesting correlations are those located off-diagonal (the cross peaks) that connect any protons that are scalarly coupled, meaning that they share a J value. These connections inform about nuclei separated by a few chemical bonds, with the intensity of the cross peak correlating with the size of the J coupling ($^2J > {}^3J > {}^4J$). Both sides of the diagonal provide equivalent information as both dimensions share the same frequency range.

Several variations of the COSY experiment have been developed over the years. One of the most popular is the COSY-45, which receives this name due to the substitution of the second ninety degree pulse by a 45° one. The reduction of this pulse length achieves a simplification of the appearance of the spectrum by reducing the autocorrelation peaks on the diagonal, allowing for observation and interpretation of cross peaks located very close to the diagonal, generated by scalarly coupled protons with small chemical shift differences. Additionally, cross peaks in the COSY-45 appear tilted and the positive/negative sign of the slope indicates the number of bonds separating the connected protons, which allows differentiation between ^2J and ^3J couplings. Other COSY variant is the DQF-COSY (Fig. 3.4b) where an extra pulse is added in the mixing step creating *double-quantum* transitions or coherences (Rance et al. 1983) (see Chap. 2 for a brief description of *double-quantum* transitions in the relaxation pathways of NOESY). Although a detailed description of these types of transitions is out of the scope of this book, it is interesting to know that the water molecule has no double-quantum transitions, which allows it to be eliminated from the DQF-COSY spectrum, while the rest of cross peaks are retained. Therefore, this sequence is specially recommended for samples dissolved in water, such as those used in biomolecular NMR. Furthermore, the DQF diagonal shows a significant reduction of the characteristic *tails* in the cross peaks that are common in the typical COSY experiment. The fine structure of the cross peaks allows for another level of interpretation.

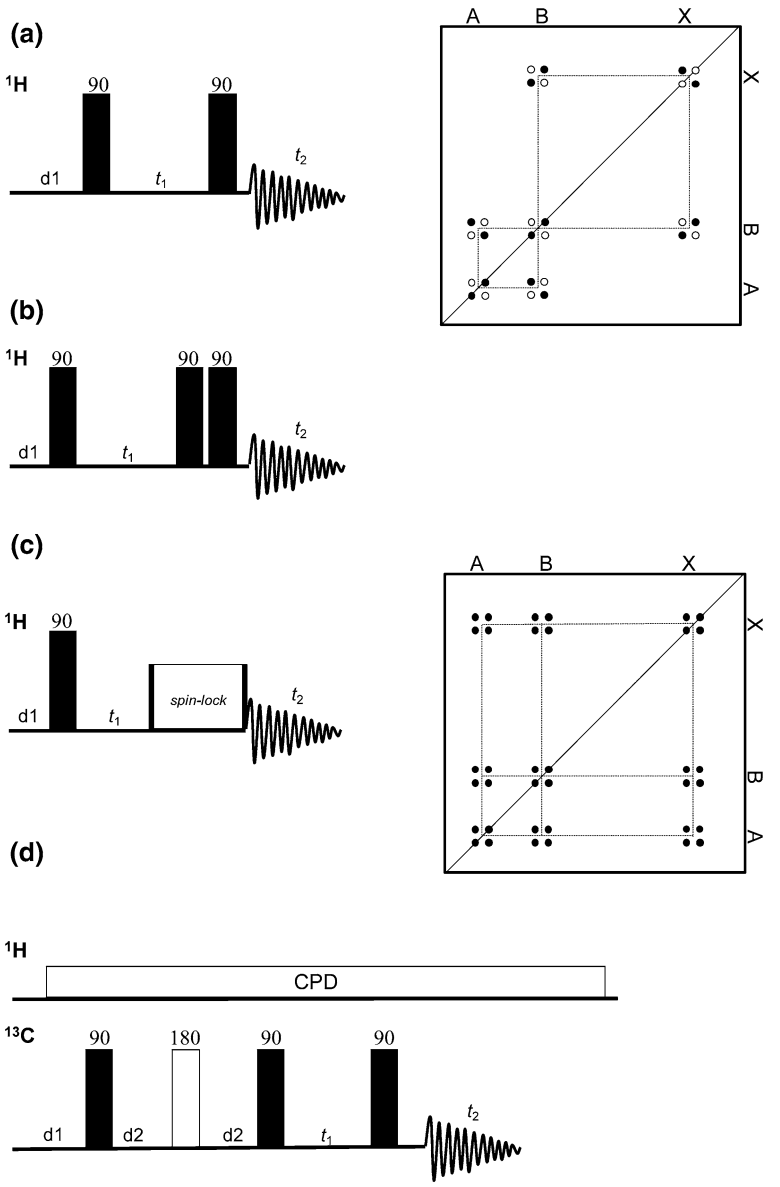

Fig. 3.4 2D homonuclear shift-correlated experiments. **a** Basic 2D ^{1}H-^{1}H COSY pulse sequence and scheme of the expected spectrum for an A-B-X spin system, where A-B and B-X are scalarly coupled but A-X are not. The pattern of the peaks in a COSY corresponds to four lobules, with alternated signs (positive and negative), due to the effect of the coupling constant among the covalently-bound nuclei. **b** DQF-COSY pulse sequence. **c** ^{1}H-^{1}H TOCSY and pattern of peaks for the A-B-X spin system. The spin-lock is achieved via a composite pulse sequence consisting in a train of several consecutive low power pulses; the pattern of peaks corresponds to a single lobule with the same sign. **d** 2D ^{13}C-^{13}C INADEQUATE sequence; it operates via the creation of multiple quantum coherences (MQC); the delay d2 is optimized for a value $1/4J_{CC}$

3.4.2 TOCSY. Practical Aspects

The TOCSY pulse sequence (TOtal Correlation SpectroscopY) (Fig. 3.4c), also known as HOHAHA (HOmonuclear HArtmann-HAhn), is a homonuclear experiment that provides a complete connection of all the protons participating in a particular spin system (Braunschweiler and Ernst 1983). The correlation is produced via scalar couplings, but in contrast to the COSY experiment which yields cross peaks only when a direct J coupling exists between nuclei, in TOCSY the correlation between spins can be observed even in the absence of a direct coupling, as long as a third spin is coupled to both. The preparation and evolution sections of the pulse sequence are identical to the COSY scheme, but they differ in the mixing stage. During the mixing period a composite pulse sequence (MLEV or DIPSI) is applied, consisting of a train of many consecutive low power pulses or *spin-lock*. This scheme makes the spins only *sense* B_1 (created by the train of pulses) as the effective field, eliminating any chemical shift differences between connected protons. During this time, the spins are *locked*, and cross peaks are produced with spins within the whole spin system. Experimentally, the duration of the spin-lock period determines how far into the spin-system the protons mix with each other, but this parameter also depends on the size of the molecule under study. Spin-lock blocks ranging between 40 and 200 ms are typical, with the shorter ones mainly used for large biomolecules and the longer ones applied to small molecules. However, it is good practice to acquire two TOCSYs with different duration in the spin-locking to account for relaxation effects in biomolecules (Cavanagh et al. 1996).

The TOCSY experiment gives more information than the COSY, as the scalar coupling information is relayed along the spin system. However, there is no way to discriminate which TOCSY peaks arise from direct coupling and which from relayed coupling. Therefore, combining the information rendered by both experiments gives the best results for the structural analysis of the molecules.

3.4.3 Correlation for Diluted Spins: The INADEQUATE Experiment. Double-Quantum Selection

Typical homonuclear experiments are not normally applied for low abundance spins such as ^{13}C because the probability of finding two carbon-13 nuclei scalarly coupled is very low and detecting their signal would require prohibitively long acquisition times. However, there are experiments that facilitate the correlation of dilute spins; among them is the INADEQUATE sequence (Incredible Natural Abundance DoublE QUAntum Transfer Experiment) (Fig. 3.4d). INADEQUATE achieves its target by creating multiple quantum coherences (MQC) between scalarly coupled spins (Freeman 1997). Multiple quantum effects can be fully grasped with quantum mechanics, however for illustrative purposes, some authors describe the MQC (Claridge 1999) within the naïve framework provided by the

vectorial model, as antiphase vectors (see the INEPT description below) which have zero net magnetization and therefore cannot be observed (as happens with the *double-quantum* sequences). Only spin-coupled systems are capable of creating MQC, in contrast to other intense signals produced by the pulse sequence which can then be filtered out. MQCs are built during the preparation stage of the pulse sequence by the application of three radiofrequency pulses separated by delays determined by J (d2), the coupling constant connecting the spins to be detected. The preparation block is followed by the evolution one and its incremental time t_1, ending with the mixing stage where a final pulse transforms the MQCs, which are not directly detectable in the NMR, into magnetization that we can observe and interpret. The cross peaks appearing in an INADEQUATE spectrum correlate with the chemical shifts of the nuclei in the horizontal (f_2) dimension, whereas the vertical (f_1) dimension represents the sum of frequencies of two spins that are coupled (Bax et al. 1980, 1981a, b; Buddrus and Bauer 1987) Although the INADEQUATE experiment is still very insensitive and can take several days of acquisition time even for very concentrated samples, it renders very valuable information for the structural characterization of molecules. It is mainly used for systems where the application of heteronuclear correlations is not possible due to the absence of sensitive nuclei such as ^{1}H or ^{31}P in the molecule. It has found its niche in the detection of ^{13}C-^{13}C connections although other low abundance nuclei can be used, and it has also found wide applications in the field of metal NMR (e.g. ^{183}W) where it is common to find molecules lacking other sensitive sources of magnetization.

3.5 Heteronuclear Shift Correlation: Correlations Through the Chemical Bond

Chemical shift values inform about the chemical environment of nuclei, and are determined by chemical bonding and spatial interactions. Together with the information extracted from spin–spin couplings, chemical structures can be established via NMR spectroscopy. However, extracting the relevant information from crowded spectra or ambiguous data can give rise to multiple valid structural possibilities, and determination of the correct one can be a far from trivial task. We have seen previously in the description of 2D homonuclear experiments like COSY or TOCSY that the interpretation of cross peaks in those spectra is much easier than in overcrowded 1D experiments, where the ambiguity of degenerate couplings and the overlap of signals can be a dead-end for molecular assignment (i.e. the atom-NMR signal equivalence). Analogous to what we have described for homonuclear experiments, heteronuclear spectra can connect different nuclei within the same experimental setup. The ^{1}H spin normally acts as the source of magnetization in these heteronuclear experiments because of its high sensitivity and omnipresence in chemical entities. Any heteronuclei can in principle be

detected using these schemes, providing a scalar coupling exists between the heteronucleus of interest and ^{1}H. However, the most common heteronuclear experiments are applied to the detection of the ^{13}C and/or ^{15}N spins (in biomolecular NMR, Chap. 4), although examples are available for most of the nuclei in the periodic table. A selection of some of the most relevant heteronuclear sequences follows. The interested reader can find more sequences in specialised texts (Muller 1979; Lerner and Bax 1986; Bax and Subramanian 1986).

3.5.1 Polarization Transfer Experiments: SPT and INEPT Sequences; Indirect Spectroscopy

The basis of all *polarization transfer* experiments is the transmission of magnetization between nuclei that are coupled. Magnetization can be transferred from a high sensitivity nucleus (e.g. ^{1}H) onto a less receptive one (e.g. ^{13}C, ^{15}N) with the aim of indirectly detecting the latter (indirect spectroscopy); the advantages of the scheme are apparent. Polarization transfer not only achieves the detection of low abundance/sensitivity nuclei but at the same time it provides chemical bonding information crucial for the assignment/identification of complex molecules. The opposite strategy (transfer from low to high sensitivity nucleus) will generate equivalent information about the system but will present evident sensitivity problems. Indirect (or inverse) spectroscopy has led to the development of most of the multidimensional experiments that are applied nowadays to medium size molecules and large macromolecules like proteins or nucleic acids. The basis of these NMR experiments is *population transfer*, which can be described as an inversion of populations of states (α and β are swapped) while observing the response from a coupled X nucleus (Fig. 3.5a). For this transfer of populations to work, a J coupling between the two nuclei is required. Although they are not currently applied as commonly as when they were first developed, the simplest population transfer schemes will be described as they constitute the building blocks from which modern pulse sequences are constructed.

3.5.1.1 SPT

In the SPT or Selective Population Transfer experiment one line in a multiplet is irradiated, altering the intensities of the lines of a second multiplet to which it is coupled (Sørensen et al. 1974; Jakobsen et al. 1974). Experimentally, this irradiation procedure is achieved via a *soft* (low power) long pulse (Fig. 3.5b). By selectively irradiating the ^{13}C satellites in the ^{1}H spectrum (arising from the ^{1}H-^{13}C coupling) and subsequently recording the ^{13}C spectrum, we shall get a net intensity gain in the ^{13}C signals. The soft pulse applied at a specific satellite resonance in the ^{1}H spectrum produces the transfer of populations, whereas the

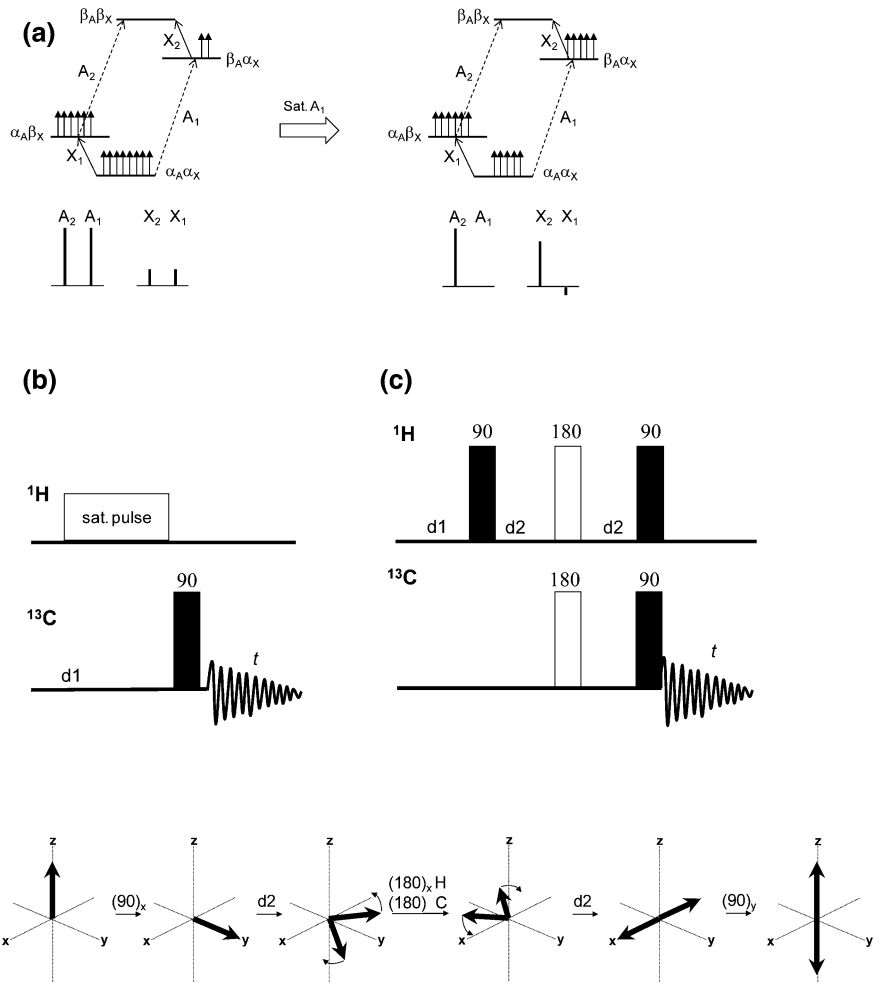

Fig. 3.5 2D heteronuclear-shift correlated experiments. **a** Energy levels, populations and expected signals for a heteronuclear AX system (e.g. ^{1}H-^{13}C) at equilibrium (*left*) and after saturation of the A1 transition (*right*). **b** ^{1}H-^{13}C Selective Population Transfer (SPT) pulse sequence. **c** ^{1}H-^{13}C INEPT pulse sequence (*top*) and vector diagram for the evolution of the proton magnetization (*bottom*). After the tilting of the proton magnetization by the first 90° pulse and its evolution during d2 ($1/4J_{CH}$) the two 180° pulses on both nuclei flip the vectors about the x-axis and invert their sense of precession. Further evolution during the second d2 leads to antiphase vectors, which are aligned along the ±z-axis by the 90° pulse on the proton. A sensitivity enhancement will be observed in the ^{13}C signals via polarization transfer

90° degree pulse on ^{13}C tilts the magnetization of the carbon nucleus that is finally observed. The ^{13}C spectrum recorded in this way will show those carbon signals coupled to the irradiated protons with increased intensities and modified multiplicities compared to a normal 1D ^{13}C spectrum, thereby allowing the

identification of those carbon atoms that are bound to the irradiated protons. By initially exciting the more sensitive of the two nuclei in the general SPT, we obtain a gain in S/N according to the formula γ_H/γ_X that in the ^{1}H-^{13}C case reaches an enhancement factor of 4 compared to the ^{13}C direct detection experiment. The SPT is of general applicability, and for nuclei with even lower γ values than ^{13}C the gain increase is larger. In the case of molecules that do not contain protons or these are not coupled to the heteronucleus of interest, the same procedure can be applied substituting the ^{1}H for other nucleus that serves as polarization source, preferably of high sensitivity (^{31}P, ^{19}F, etc.).

3.5.1.2 INEPT

The INEPT sequence (Insensitive Nuclei Enhanced by Polarization Transfer) (Fig. 3.5c) results in a significant improvement over the simpler SPT and its development in the late seventies in the group of Ray Freeman opened the way for the subsequent development of the multidimensional heteronuclear experiments (Morris and Freeman 1979). INEPT does not employ selective polarization on individual signals as is applied in SPT, but instead it uses hard radiofrequency pulses with the aim of exciting the whole frequency range of the nucleus and achieving all possible population transfers in one single experiment. In this way the selection and precise irradiation of signals is avoided. As before, the existence of a *J* coupling between nuclei is needed for the experiment to produce its outcome, which is to observe the signals from the heteronuclei with a significant sensitivity enhancement by the transfer of populations from a more sensitive nucleus, normally the proton.

Although the number of pulses is increased in comparison with SPT, the INEPT maintains a very simple scheme. The first 90° pulse is applied on the more sensitive nucleus, creating transverse magnetization in the xy-plane. Two delays optimized to a length d2 = 1/4 *J*, *J* being the scalar coupling between ^{1}H and X, are located at both sides of the 180° pulses applied simultaneously on both nuclei. During these two d2 delays both the ^{1}H-X spin coupling and the chemical shift evolve, but the latter is refocused by the 180° applied on the proton frequency, whereas the 180° on X modulates the spin-echo (similar to those described in Chap. 1 to measure the T_2). At the end of the second d2 delay the sequence has developed antiphase magnetization of the proton with respect to the coupled carbon, which is converted into ^{13}C antiphase magnetization by the two final 90° pulses, finally evolving into in-phase ^{13}C magnetization (detectable signal) during the FID. In short, with the INEPT scheme we shall achieve in the first place transfer of magnetization from the sensitive (^{1}H) to the insensitive nucleus (X) resulting in a net gain of S/N, and secondly we shall obtain X resonances with splittings arising from *J* couplings to the protons, their sizes and multiplicities revealing relevant structural information. No decoupling scheme is applied in the INEPT experiment to preserve the couplings. The increase in sensitivity is

equivalent to that obtained with the SPT experiment (γ_H/γ_X) and independent of the sign of gamma.

Although the basic INEPT experiment is not usually applied on its own nowadays, its five-pulse building block is extensively used in more complicated multidimensional experiments where heteronuclear population transfer is required (HSQC and related experiments; see Sect. 3.5.2). Some INEPT variants have been developed, among them the reverse-INEPT (Freeman et al. 1981), where the population transfer goes from X to ^{1}H. Although applying the starting pulse on the insensitive X nucleus may seem counterproductive, it has the advantage that the final detection, and therefore the main source of sensitivity, is on the ^{1}H. The final spectrum will be a 1D ^{1}H, showing antiphase proton signals split according to the couplings with the heteronucleus. Hardly used in routine NMR on its own, the reverse-INEPT block of pulses is frequently used as a method to return magnetization from X to ^{1}H in more complex pulse sequences.

3.5.1.3 DEPT

The DEPT (Distortionless Enhancement by Polarization Transfer) is another experiment based on polarization transfer (Ernst et al. 1987; Doddrell et al. 1982) that is generally applied for spectral editing (selection or differentiation of NMR signals according to their chemical nature), as it provides a sign differentiation of the heteronuclei resonances according to the number of attached protons; in general terms, it can be considered an improved version of the INEPT experiment. It follows the typical scheme based on the magnetization transfer from the protons to the X heteronucleus, but it relies now on a selected flip angle of one of the pulses which will determine the sign of the X(H)n resonances. Largely, it has been applied for the differentiation of CH, CH_2, CH_3 and quaternary carbons (absent in the DEPT) in ^{13}C spectra. The most used variant is DEPT-135 (flip angle = 135°) that provides positive signals for the CH and CH_3 carbons and negative for the CH_2. With a straightforward superimposition with the typical 1D ^{13}C spectrum from the same molecule, a quick identification of the carbon multiplicities can be easily carried out.

3.5.2 Heteronuclear Single-Bond Correlations: HSQC and HMQC

The HSQC (Heteronuclear Single Quantum Coherence) (Bodenhausen and Ruben 1980) and HMQC (Heteronuclear Multiple Quantum Coherence) (Bax et al. 1983, 1990; Norwood et al. 1990) pulse sequences are two of the most applied experiments in routine NMR. Although obtained through different pathways, the information they provide is equivalent: a single-bond correlation between a sensitive

nucleus, most commonly ^{1}H, with the heteronucleus of interest (e.g. ^{13}C, ^{15}N). For example, the ^{1}H-^{13}C heteronuclear correlation combines in a single experiment the chemical shift information contained in the corresponding 1D ^{1}H and ^{13}C spectra, plus the connection between the protons and the carbon to which they are bound. Indirectly, the correlation allows the identification of those protons in the molecule not bound to a carbon atom (e.g. NH, OH) and carbons with no attached proton (quaternary carbons). Together with the homonuclear experiments described before, these heteronuclear correlations are an essential tool in the structural analysis of any molecule, independent of their size and complexity.

The basic 2D HMQC experiment (Fig. 3.6a) shows a remarkable simplicity with only four radiofrequency pulses. The preparation part of the sequence includes a 90° pulse on each of the frequency channels (^{1}H and X), separated by a delay d2 optimized to 1/2 J, where J is the average one-bond ^{1}H-X scalar coupling. This building block achieves the creation of the multiple quantum coherences (MQC) between any two coupled spins that give name to the sequence. In the middle of the evolution time t_1 there is a 180° pulse on the ^{1}H channel that removes multiple quantum frequencies corresponding to ^{1}H chemical shifts, leaving undisturbed any ^{1}H-^{1}H coupling as well as the ^{1}H-X MQCs. The final 90° pulse on the X channel returns the ^{1}H-X MQ coherences to magnetization we can actually observe, with the FID being acquired at the ^{1}H frequency contrary to X-detection of the polarization transfer sequences (SPT, INEPT, DEPT) described before (Fig. 3.5). The application of the initial pulse on the sensitive ^{1}H nucleus and its detection on the same channel at the end of the sequence increases dramatically the sensitivity of the HMQC compared to the INEPT-type sequences. Although the HMQC generates one-bond correlations with high S/N, the detected signals are in antiphase and split due to the homonuclear ^{1}H-^{1}H couplings evolving during t_1. To obtain fully absorptive signals, the HMQC is normally processed in magnitude mode (i.e. absolute value), removing any sign discrimination but also significantly broadening the resonance peaks.

Although the HMQC experiment was originally designed for the correlation of one-bond heteronuclear couplings, the delay d2 can be adjusted to detect any long-range ^{1}H-X ^{n}J. However, the evolved ^{1}J couplings will also appear on the 2D spectrum adding complexity to the molecular characterization. To be able to discriminate long-range correlations from one-bond ones, a variant of the HMQC called HMBC (Heteronuclear Multiple Bond Correlation) (Fig. 3.6b) (Bax and Summers 1986; Summers et al. 1986) has been developed. By adding a few extra pulses and delays but maintaining the simplicity of its HMQC source, the HMBC achieves the generation of heteronuclear correlations up to several bonds as far as there is a measurable scalar coupling. The two additional pulses at the beginning of the sequence act as a *low-pass* filter that is responsible for the elimination of the potentially disturbing ^{1}J correlations. Combined with the results from the simple ^{1}J HMQC, the connecting information obtained in the HMBC normally ensures the full structural assignment of small to medium sized molecules. As in the HMQC sequence, antiphase magnetization originated from the heteronuclear couplings enters the acquisition time; no refocusing or decoupling are included in

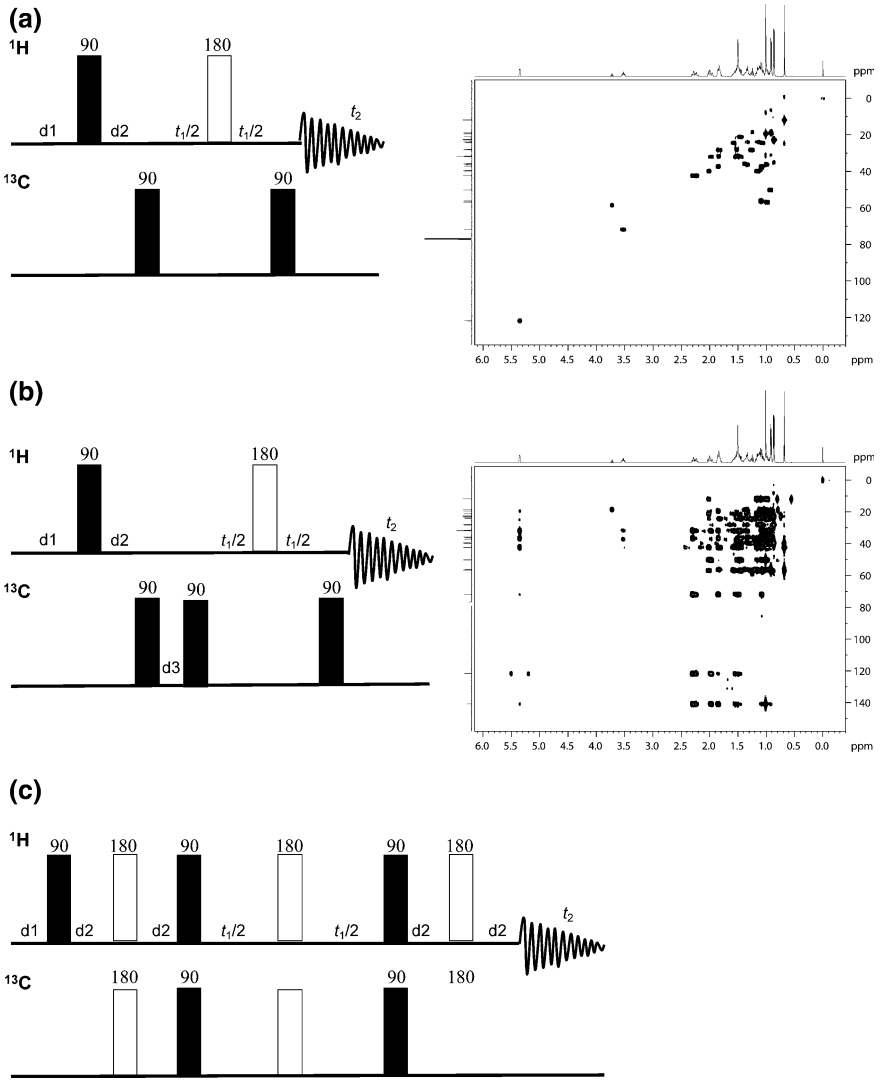

Fig. 3.6 2D heteronuclear-single bond correlations. **a** HMQC sequence and spectrum of cholesterol; d2 is optimized to $1/2{}^{1}J_{CH}$. **b** HMBC sequence and spectrum of cholesterol; d2 is optimized to $1/2{}^{1}J_{CH}$ and d3 to $1/2{}^{n}J_{CH}$. **c** HSQC sequence: d2 is optimized to $1/4{}^{1}J_{CH}$

the experiment, as the diversity of couplings contributing to the FID makes it difficult to attain a full refocusing of the magnetization and the decoupling would lead to severe loss of information.

The HSQC (Heteronuclear Single Quantum Coherence) uses a slightly different approach to achieve single-bond correlations between ^{1}H and any heteronucleus (Fig. 3.6c) (Bodenhausen and Ruben 1980). The HSQC scaffold might initially

appear more complex than the HMQC experiment, but it can be deconvoluted into INEPT and retro-INEPT blocks separated by a 180° pulse in the middle of the evolution time. The starting INEPT block generates single quantum coherences (SQC) between ^{1}H-X that evolve during t_1. An important characteristic of the SQC is that no homonuclear ^{1}H-^{1}H couplings can evolve, in contrast to what happens in the HMQC. The chemical shift of the heteronucleus X also evolves during t_1, while the ^{1}H-X coupling is refocused by the 180° pulse. The HSQC cross peaks are not split or broadened by homonuclear couplings and can be detected in phase-sensitive mode; therefore, in terms of resolution it is superior to the HMQC experiment. This is of particular interest in large molecules with very overcrowded spectra, such as biomolecules. In fact, the ^{1}H-^{15}N HSQC experiment is almost mandatory in any protein study by NMR.

In both the HMQC and HSQC experiments, the initial excitation (first radio-frequency pulse) of the magnetization is always performed on the more sensitive of the two nuclei, normally the ^{1}H. The final detection is on the same nucleus, achieving very high sensitivity gains, especially if very-low gamma X-nuclei are to be observed. However, ^{1}H is not the only possibility for a magnetization source and, if needed, the transfer of polarization can be performed via other nuclei, preferably of high sensitivity like ^{31}P or ^{19}F. Apart from the sensitivity gain, the design of both sequences situates the heteronucleus chemical shift range in the f_1 dimension, which necessitates fewer acquisition points. This set-up is more convenient than the inverse because the X signals are generally well dispersed, requiring less resolution to define the resonances properly. This leaves the f_2 dimension with a larger allocation of points for the ^{1}H signals, which are usually crowded. The kind of information heteronuclear correlation experiments provide and the differences they present in terms of signal resolution is shown in several of the references (Norwood et al. 1990; Bax et al. 1990).

3.5.3 *Double Resonance Experiments: Homonuclear Spin Decoupling; Heteronuclear Double Resonance and Broadband Decoupling*

In Chap. 2 we described the concept of decoupling (Sect. 2.2.4) and we have used this notion in previous pulse sequence descriptions. Suppression of the scalar *J* coupling between spins by the application of a very strong radiofrequency field achieves a single line resonance. Decoupling is commonly used in ^{13}C experiments and heteronuclear correlations to increase the sensitivity of the signals by collapsing multiplets, but the application of selective homonuclear ^{1}H-^{1}H decoupling can also be used to identify connecting protons. In this case, irradiation of an individual multiplet in the ^{1}H spectrum will eliminate the splitting of that signal as well as corresponding couplings of any other ^{1}H resonances to which it is connected (see, for instance, the spectrum of ethanol in Fig. 2.1). This experiment thus

identifies proton–proton connections, although its application for molecular characterization has been superseded by techniques like COSY/TOCSY. Nowadays homonuclear decoupling is mainly applied to simplify multidimensional spectra and increase S/N. Experimentally, decoupling is achieved by irradiating at a specific ^{1}H frequency with a low-power, restricted frequency-range pulse known as a *soft* pulse, while the spectrum is acquired using the typical *hard* radiofrequency pulse. Two ^{1}H irradiation frequencies cohabit in the same experiment, giving rise to the name *double resonance*: one generating the full spectrum, applied in the middle of the chemical shift range, and a second selective frequency applied at the specific signal whose multiplicity, and that of its coupled partners, we aim to suppress.

Analogous to the selective decoupling we have just described, it is possible to achieve a decoupling scheme that affects a whole range of frequencies for a given nucleus. This is useful when no structural or coupling information is sought, but rather a raw increase in the simplicity and intensity of the resonances. Removing the splitting of signals simplifies multidimensional spectra dramatically, which is particularly important if there is a risk of cross-peak overlap. By applying the decoupling, a general increase in sensitivity is achieved via two mechanisms: the collapse of multiplets into singlets and the NOE effect between spins (Chap. 2). Experimentally, decoupling consists of a *train* of pulses applied in a very short time. Modern decoupling schemes have been designed to compensate for B_1 miscalibration and are especially robust to non-ideal conditions so they work well without particular set-up requirements. Depending on the nucleus to be decoupled, the extent of the frequency range and the spectrometer field, several multi-composite pulse sequences are usually applied. Among them, some of the most commonly used are WALTZ-16, GARP, MLEV-16 or WURST (Freeman 1997).

3.6 Correlations Through Space

So far we have introduced several NMR experiments based on scalar coupling connections transmitted via the chemical bond. However, coupling interactions between spins also exist that occur through space: the dipolar couplings. The nuclear Overhauser effect or NOE, introduced in Chap. 2, is a result of such dipolar couplings and is at the basis of many NMR experiments. The importance of the NOE in structure elucidation by NMR is unique, since it informs about the three-dimensional molecular geometry. In this section, we describe two different methods to observe the NOE: steady-state and kinetic NOE. Which one to choose will be dictated by the size of the molecule under study (Neuhaus and Williamson 1999).

3.6.1 Steady-State NOE

In the simplest NOE 1D difference experiment (Fig. 3.7a), firstly we irradiate a ^{1}H signal to reach saturation and observe the effects on all the protons dipolarly coupled to it (i.e. spatially close). The signal saturation is attained by irradiating selectively at the frequency of the chosen signal with a continuous wave of radiofrequency instead of a hard pulse, and measuring the effect thus produced with the acquisition of a ^{1}H spectrum by the application of a 90° pulse. In a second accompanying experiment, the pulse sequence is repeated but shifting the frequency of irradiation to a region of the spectrum without signals, so no NOE effect will be produced and the ^{1}H will show no signal enhancement. The difference between these two 1D spectra will yield only those resonances that see an enhancement in their intensities due to the initial NOE effect. In practical terms, this experiment is very useful to resolve the topology of a molecule and identify which protons are close in space. It can also provide structural information between fragments of a molecule that are not connected via the scalar-coupling based experiments.

This *steady-state* NOE (η) (from the steady state population distribution created via cross-relaxation of dipolarly coupled spins counteracted by their return to equilibrium) is dependent on the γ of the nuclei involved $\eta_{max} = 1/2(\gamma_A/\gamma_X)$, a characteristic that becomes relevant when the interacting spins are different. Although structurally-aimed heteronuclear NOE experiments are applied to some extent, the heteronuclear NOE is normally used as a sensitivity enhancement

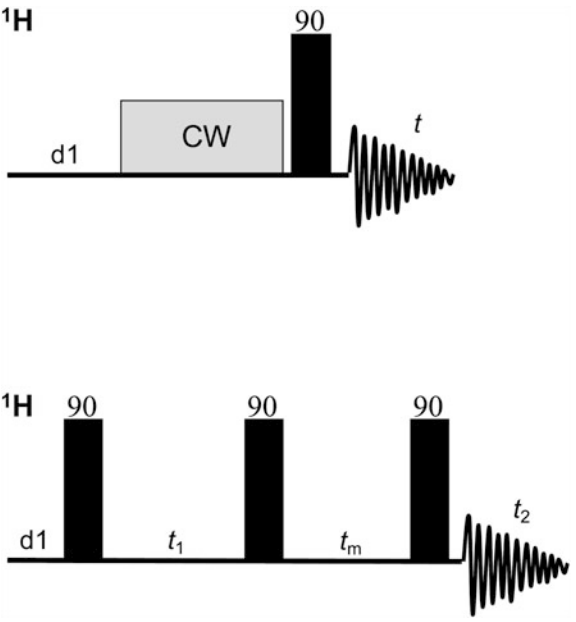

Fig. 3.7 Correlations through space. **a** Pulse sequence of the NOE 1D-difference experiment. **b** Pulse sequence of the homonuclear 2D NOESY experiment

method via broad decoupling in experiments such as 1D ^{13}C, DEPT or those described in Sect. 3.5.3. Finally, it is important to bear in mind that the sign of γ is relevant in the above discussion, and therefore the NOE effect will be negative for nuclei of $\gamma < 0$ (e.g. ^{15}N, ^{29}Si, ^{119}Sn, etc.). Depending on the size and molecular tumbling of the molecule under study, a η_{max} near -100 % could be achieved for those $\gamma < 0$ nuclei, rendering a null signal instead of the NOE enhancement expected.

3.6.2 Kinetic or Transient NOE

NOE enhancement can also be achieved by initially creating a general perturbation on a molecule via radiofrequency pulses and leaving the system to evolve in the absence of any other perturbation. In this way, the spins will relax with each other and the NOE progressively builds up until a maximum is reached from where it decays back to zero. This *kinetic* NOE experiment, also called *transient* NOE, is the foundation of the NOESY experiment shown in Fig. 3.7b. The first two 90° pulses separated by the evolution time t_1 create the conditions for the spins to be aligned on the z-axis, and during mixing time, t_m, they will relax with each other and give rise to the NOE build-up. With the final 90° pulse the magnetization is returned to the xy-plane where it can be acquired. The resulting spectrum will show all possible NOE correlations within a molecule in a single experiment (see Fig. 4.3c for the NOESY spectrum of a protein).

Molecules are multi-spin systems, and therefore, the NOE effect on a single proton cannot be isolated from all its surrounding atoms. This circumstance leads to the issue of *indirect* effects on the NOE: the NOE enhancement produced on nucleus B by the proximity of A will be conveyed to nucleus C that is close to B but not to A. An NOE will be observed between A and C, even though they are not close enough in space to produce it. These indirect effects between nuclei that are further apart than the maximum distance to generate NOE connections are a consequence of long mixing times in the pulse sequence. In the case of small molecules these indirect NOEs have different sign to the direct NOEs and can therefore be easily identified. However, for large molecules such as proteins there is no sign difference between direct and indirect NOEs, which can become a serious problem when performing internuclear distance analysis.

This indirect effect is also known as *spin diffusion.* Although it is almost unavoidable, its presence can be discerned by acquiring experiments with increasing mixing times, thereby presenting different NOE build-up rates (the shorter the mixing time the less spin diffusion we will observe). The rate of growth of the NOE is directly related to the internuclear distance between spins by an r^{-6} factor. If the intensity of a specific NOE signal is linked to a known internuclear distance in the molecule (e.g. based on an X-ray structure or from an assigned secondary structure in a biomolecule), this cross peak calibration will give us a reasonable distance-range *versus* intensity correlation for the rest of resonances in the spectrum.

The relevance of this relationship between NOE intensity and internuclear distances will become clear in the next chapter, dedicated to biomolecules.

3.6.3 The 2D NOESY Sequence and Practical Aspects of the Experiment

The 2D NOESY experiment is normally applied to large molecules such as proteins or nucleic acids and follows the usual scheme for a multidimensional experiment. The mixing time during which the transient NOEs between spins develop is usually in the range of 50–300 ms, depending on the size of the molecule (as a rule of thumb, the larger the molecule the shorter the mixing time). The main features of the spectrum are similar to those seen for COSY or TOCSY, with the central difference that in the NOESY experiment the cross-peaks represent two nuclei located at distances no greater than 5–6 Å. Although spin diffusion is always present and needs to be taken into account, the intensities can be correlated with internuclear distances (r^{-6}), bearing in mind that the intensity of the NOE peak is contributed by all surrounding protons, with the nearest ones contributing to a larger extent.

As we already pointed out in Chap. 2, for medium-sized molecules η_{max} goes from positive to negative values in the region of intermediate molecular tumbling. The correlation time depends on the size and shape of the molecule, the viscosity of the solvent and the temperature of acquisition but there is a real risk that the NOESY experiment yields none or hardly any NOE enhancements for a significant range of molecules. In these cases the use of the alternative ROESY (Rotating frame Overhauser Effect SpectroscopY) sequence is recommended (Neuhaus and Williamson 1999). This experiment makes use of a spin-lock scheme like that applied in the TOCSY, but of weaker strength, that is able to generate a similar rotating frame Overhauser effect or ROE. Under these experimental conditions the NOE/ROE is always positive and the near-zero enhancement is no longer an issue.

References

Aue WP, Bartholdi E, Ernst RR (1976) Two-dimensional spectroscopy. Application to nuclear magnetic resonance. J Chem Phys 64:2229–2246

Bax A, Freeman R (1981) Investigation of complex networks of spin–spin coupling by two-dimensional NMR. J Magn Reson 44:542–561

Bax A, Freeman R, Kempsell SP (1980) Natural abundance C-13–C-13 coupling observed via double quantum coherence. J Am Chem Soc 102:4849–4851

Bax A, Freeman R, Frenkiel TA, Levitt MH (1981a) Assignment of carbon-13 NMR spectra via double-quantum coherence. J Magn Reson 43:478–483

Bax A, Freeman R, Frenkiel TA (1981b) An NMR technique for tracing out the carbon skeleton of an organic molecule. J Am Chem Soc 103:2102–2104

Bax A, Griffey RH, Hawkins BL (1983) Correlation of proton and nitrogen-15 chemical shifts by multiple quantum NMR. J Magn Reson 55:301–315
Bax A, Ikura M, Kay LE, Torchia DA, Tschudin R (1990) Comparison of different modes of two-dimensional reverse correlation NMR for the study of proteins. J Magn Reson 86:304–318
Bax A, Summers MF (1986) Proton and carbon-13 assignments from sensitivity-enhanced detection of heteronuclear multiple-bond connectivity by 2D multiple quantum NMR. J Am Chem Soc 108:2093–2094
Bax A, Subramanian S (1986) Sensitivity-enhanced two-dimensional heteronuclear shift correlation NMR spectroscopy. J Magn Reson 67:565–569
Buddrus J, Bauer H (1987) Determination of the carbon skeleton of organic compound by double-quantum coherence carbon-13 NMR spectroscopy—the INADEQUATE pulse sequence. Angew Chem Int Ed Engl 26:625–642
Berger S, Braun S (2003) 200 and more NMR experiments. Wiley-VCH, New York
Bodenhausen G, Ruben DJ (1980) Natural abundance nitrogen N-15 by enhanced heteronuclear spectroscopy. Chem Phys Lett 69:185–189
Braunschweiler L, Ernst RR (1983) Coherence transfer by isotropic mixing: application to proton correlation spectroscopy. J Magn Reson 53:521–528
Claridge TDW (1999) High-resolution NMR techniques in organic chemistry. Pergamon Press, Oxford
Cavanagh J, Fairbrother WJ, Palmer AG 3rd, Skelton N (1996) Protein NMR spectroscopy. Principles and practice, 1st edn. Academic Press, New York
Derome AE (1987) Modern NMR techniques for chemistry research. Pergamon Press, Oxford
Doddrell DM, Pegg DT, Bendall MR (1982) Distorsionless enhancement of NMR signals by polarization transfer. J Magn Reson 48:323–327
Ernst RR, Bodenhausen G, Wokau A (1987) Principles of NMR in one and two dimensions, Chapter 4. Clarendon Press, Oxford
Freeman R (1997) Spin choreography: basic steps in high resolution NMR. Spektrum, Oxford
Freeman R, Mareci TH, Morris GA (1981) Weak satellite signals in high resolution NMR spectra: separating the wheat from the chaff. J Magn Reson 42:341–345
Hoch JC, Stern AS (1996) NMR Data Processing. Wiley-Liss, New York
Jakobsen HJ, Linde SA, Sørensen S (1974) Sensitivity enhancement in ^{13}C FT NMR from selective population transfer (spt) in molecules with degenerate proton transitions. J Magn Reson 15:385–388
Jeener J (1971) Ampere International Summer school. Basko Polje, Yugoslavia
Lerner L, Bax A (1986) Sensitivity-enhanced two-dimensional heteronuclear relayed coherence transfer NMR spectroscopy. J Magn Reson 69:375–380
Morris GA, Freeman R (1979) Enhancement of nuclar magnetic resonance signals by polarization transfer. J Am Chem Soc 101:760–762
Muller L (1979) Sensitivity enhanced detection of weak nuclei using heteronuclear multiple quantum coherence. J Am Chem Soc 101:4481–4484
Neuhaus D, Williamson MP (1999) The nuclear Overhauser effect in structural and conformational analysis, 2nd edn. VCH Publishers, New York
Norwood TJ, Boyd J, Heritage JE, Soffe N, Campbell ID (1990) Comparison of techniques for proton detected 1H–15 N spectroscopy. J Magn Reson 87:488–501
Parella T (1999) NMR guide. Bruker, Karlsruhe
Rance M, Sørensen OW, Bodenhausen G, Wagner G, Ernst RR, Wüthrich K (1983) Improved spectral resolution in cosy 1H NMR spectra of proteins via double quantum filtering. Biochem Biophys Res Commun 117:479–485
Sørensen S, Hansen RS, Jakobsen HJ (1974) Assignments and relative signs of ^{13}C-X coupling constants in ^{13}C FT NMR from selective population transfer. J Magn Reson 14:243–245
Summers MF, Marzilli LG, Bax A (1986) Complete proton and carbon 13 assignments of coenzyme B12 through the use of new two-dimensional experiments. J Am Chem Soc 108:4285–4294